30th Annual International IEEE EMBS Conference
Vancouver, British Columbia, Canada, August 20-24, 2008

Development of Failure Detection System Based on Vibration Signal for Smart Artificial Heart: in Vitro Study

Shinichi Tsujimura, Takashi Kuwabara, Harutoshi Koguchi, Takashi Yamane,
Tatsuo Tsutsui, and Yoshiyuki Sankai

Abstract— **To realize safe and effective medical treatment for patients with implantable artificial hearts, we have developed a smart artificial heart (SAH). The SAH can grasp the mechanical condition of the artificial heart and the physiological condition of the patient. The purpose of this study is to develop a failure detection system based on the vibration signal from artificial heart in order to enhance the ability of failure detection for the SAH. We suppose this vibration signal reflects not only the mechanical condition of the artificial heart but also a part of the physiological condition of the patient. The developed failure detection system is composed of a vibration sensor unit and a failure detection algorithm. The algorithm has a standard frequency pattern, which is made from the vibration signal of good condition of both the artificial heart and patient. Observing the difference from the standard frequency pattern, the algorithm detects failure conditions. Therefore, this algorithm does not need prior knowledge of vibration characteristics corresponding to failures. After confirming that the vibration signal are affected by pump speed and pulsation in two kinds of mock circulatory loops, we performed thrombogenesis detection by using the failure detection system in mock circulatory loop with sheep blood. As a result, this system indicated a possibility of detecting the initial sign of thrombogenesis earlier than current signal. In conclusion, we think that this failure detection system can cooperate with other sensor systems of the SAH and enhance the ability of failure detection for the SAH.**

I. INTRODUCTION

The development of the artificial hearts has made great strides over the past few years. Centrifugal blood pumps especially have been developed for the purposes of their small size, high efficiency, and simple design from the viewpoint of hardware [1-3]. To guarantee the patient's more long-term saftey, it is essential to manage both the physiological condition of patients with an artificial heart and the driving condition of the artificial heart. However, the method of measurement used in intensive care unit (ICU) is invasive and cannot be applied to the implanted artificial heart. In our laboratory, we have developed a sensorized and intelligent artificial heart called smart artificial heart (SAH) in order to realize safe and effective medical treatment as if the patients were in the ICU [4].

The SAH is shown in Fig.1. The SAH can measure not only the driving data of the artificial heart but also physiological data of the patient by small-sized, accurate, and non-invasive sensors. When the SAH is implanted into the body of the patient, these sensors never touch blood in the pump directly. Therefore the invasiveness to the human body is reduced to the minimal as much as possible. Moreover, The SAH can detect failures as one of its intelligent functions when the values of data measured with those sensors exceed predetermined threshold values. Although the SAH can detect failures after the failures became serious, it is essential to detect predictors of failure before the failure become serious. If these failures can be found during early stages and be appropriately treated, the patients can decrease their anxiety to the unexpected failure.

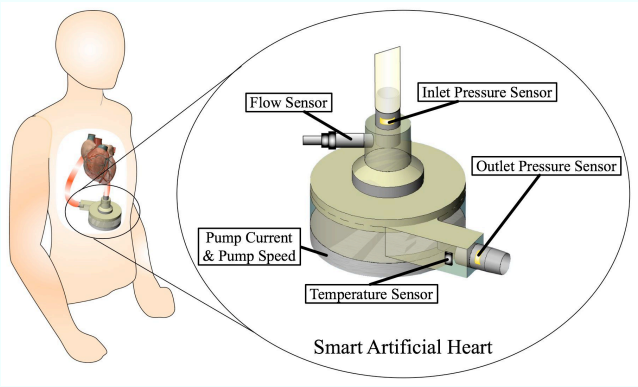

Fig. 1. Illustration of smart artificial heart with the sensors

The centrifugal blood pumps have an impeller in their structure. We suppose that the mechanical action of the impeller is affected by not only the pump's mechanical condition but also the physiological condition such as a cardiac function of the patient with the pump. Therefore, we focus on the vibration generated from the mechanical action of the impeller. Failure detection using vibration signals has advantages as follows: availability of small-sized vibration sensor, noninvasive measurement, and simple system design. These advantages are suitable to the SAH. Several studies have already reported failure detection method using frequency analysis of vibration signal in centrifugal pumps [5], [6]. These studies show the effectiveness of failure detections by using the proposed methods. However, it is difficult to apply these methods to the implanted artificial heart.

The purpose of this study is to develop a failure detection system based on the vibration signals from artificial heart in order to enhance the ability of failure detection for the SAH.

Shinichi Tsujimura, Takashi Kuwabara, Harutoshi Koguchi, and Yoshiyuki Sankai are with Systems and Information Engineering, University of Tsukuba, 1-1-1 Tennoudai, Tsukuba, Ibaraki, 305-8573, Japan (e-mail: tujimura@ golem.kz.tsukuba.ac.jp

Takashi Yamane is with the National Institute of Advanced Industrial Science and Technology, Tsukuba, Japan.

Tatsuo Tsutsui is with the Institute of Clinical Medicine, University of Tsukuba, Japan.

978-1-4244-1815-2/08/$25.00 ©2008 IEEE.

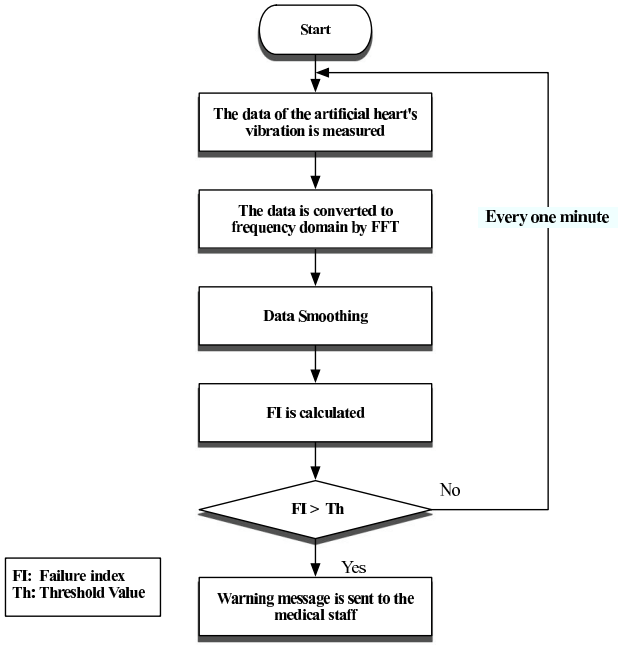

Fig. 2. Flow chart of failure detection algorithm

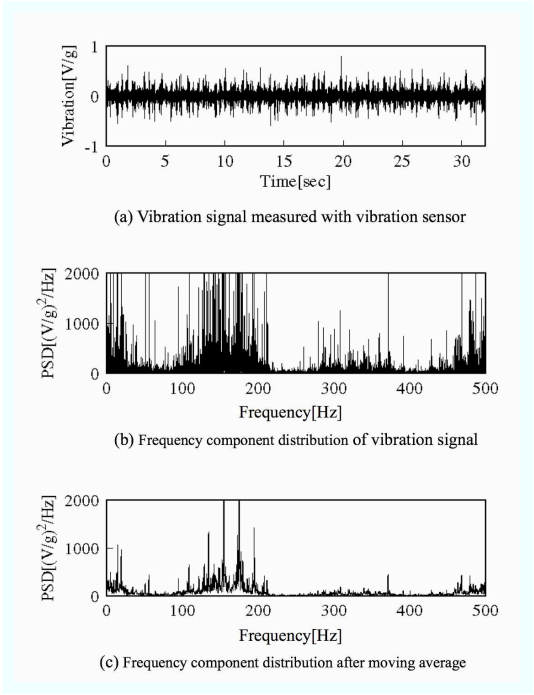

Fig. 3. Waveforms according to the processes in Fig. 2

II. MATERIALS AND METHODS

A. Failure detection system

An failure detection system consists of a vibration sensor unit and a personal computer with a failure detection algorithm. The vibration sensor unit is composed of a vibration sensor, an amplifier, and an anti-aliasing filter. The vibration sensor was selected according to the shape of centrifugal blood pumps. The flow chart of the proposed failure detection algorithm is shown in Fig. 2. In order to detect failures occurring rapidly, this algorithm continuously calculated a failure index every one minute. Moreover, a warning message was sent when the value of the failure index exceeded the threshold decided previously. The value was calculated as follows.

Firstly, vibration signals from an artificial heart were measured using the vibration sensor. Moreover, the signals were saved to a personal computer (PC) via the data recording device with 14 bit resolution analog-to-digital converter. The vibration signals are shown in Fig. 3(a).

Secondary, to make frequency pattern of the signals, we applied fast Fourier transform (FFT) with the Hamming window to discrete Fourier transform (DFT) in the PC. The equation of the DFT is shown as follows:

$$F(i) = \sum_{x=0}^{N-1} f(x) e^{\frac{-j2\pi ix}{N}} \tag{1}$$

$$i = 0, 1 \cdots, N-1$$

where $f(x)$ is the measured vibration data. $F(i)$ is frequency spectrum data. The frequency spectrum data of N points were calculated using Octave as numerical analysis software. In the range of over 0 Hz, the power spectrum density (PSD) of $F(i)$ is shown in Fig. 3(b).

Thirdly, to extract the features of the frequency pattern, we calculated moving average of the frequency pattern by the following mathematical equation:

$$P^{'}(m) = \frac{1}{2s+1} \sum_{k=-s}^{s} P(m+k) \tag{2}$$

$$m = 0, 1 \cdots, \frac{N}{2} - 1$$

where $P(m)$ is PSD of $F(i)$ in the range of over 0 Hz. $P^{'}(m)$ is result calculated by using moving average. The result of the moving average is shown in Fig. 3(c). Finally, we calculated a correlation coefficient between a standard frequency pattern and a present frequency pattern. This correlation coefficient is result of the pattern matching. We calculated the correlation coefficient and derived the failure index by the following mathematical equation:

$$R = \frac{m\sum P_n P_c - (\sum P_n)(\sum P_c)}{\sqrt{(m\sum P_n^2 - (\sum P_n)^2)(m\sum P_c^2 - (\sum P_c)^2)}} \tag{3}$$

where P_n is the given normal standard frequency pattern. P_c is the present frequency pattern. m is the number of P(m). R is the correlation coefficient. We defined the failure index from R as follows:

$$failure\ index = \begin{cases} |\ R-1| & R \geq 0 \\ 1 & R < 0 \end{cases} \tag{4}$$

When the failure index approaches 0, the present frequency pattern approaches the standard frequency pattern. Conversely, when the failure index approaches 1, the present

frequency pattern differs from the given standard frequency pattern. In other words, the failure index increases within the range of 0 to 1 according to the degree of failure. The feature of this algorithm is to compare the present frequency pattern with the standard frequency. We can turn up an unknown frequency pattern which is different from the given standard frequency pattern. Consequently, the developed failure detection system can detect the failure condition affecting the mechanical action of the pump impeller without any prior knowledge related to vibration characteristics corresponding to failures.

B. Experiments

We investigated the mechanical action of the impeller in a centrifugal blood pump by using a part of the developed system in two mock circulatory loops. Furthermore, we performed thrombogenesis detection by using the failure detection system in mock circulatory loop with sheep blood. Through these experiments, the pump speed was set to under 2000 rpm (about 33 Hz), thus we thought the sampling frequency of vibration signal was over 400 Hz. Considering the mechanical frequency response of vibration sensor attached centrifugal blood pumps, we decided the sampling frequency of vibration signal was set to 1k Hz or 400 Hz. To calculate the failure index every one minute, the FFT window size was set to 16384 points (about 41 sec) in case of 400 Hz sampling and was set to 32768 points (about 33 sec) in case of 1 kHz sampling.

1) Investigation of frequency pattern affected by pump speed: In this experiment, we investigated the frequency pattern of the vibration signal affected by the pump speed. The mock circulatory loop was constructed as shown in Fig. 4. This mock circulatory loop consists of the centrifugal blood pump with double-pivot bearing (Gyro-Pump, Kyocera Co., Kyoto, Japan), and the reservoir. The circulation loop was filled with water as working fluid. The vibration sensor with the mechanical frequency response up to 500 Hz was mounted near the outlet port of the pump. The pump speed was set to 1400 rpm, 1600 rpm, 1800 rpm, and 2000 rpm. At that time, the pump flow and the vibration signals were measured and saved by using the computer via the data recording device at 1 kHz sampling. The data points for FFT were 32768 points. The pressure differences across the pump were derived from the pump speed, the pump flow, and the head-capacity curve of the pump.

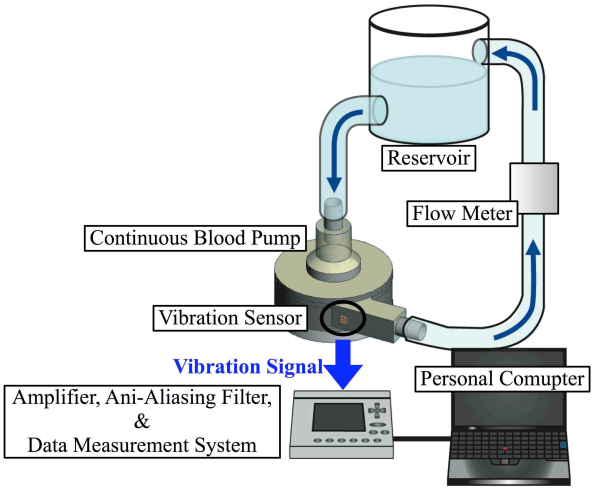

Fig. 4. Mock circulatory loop for investigation of frequency pattern affected by pump speed

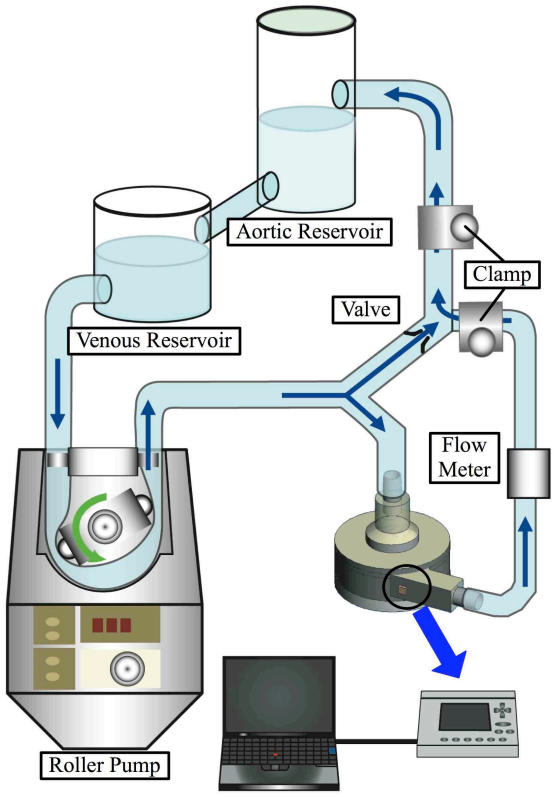

Fig. 5. Mock circulatory loop for Investigation of frequency pattern affected by pulsation

2) Investigation of frequency pattern affected by pulsation: In this experiment, we investigated the frequency pattern of the vibration signal affected by the pulsation. The mock circulatory loop was constructed as the systemic circulation loop as shown in Fig. 5. This mock circulatory loop consists of the same centrifugal blood pump used, the roller pump making pulsation instead of the natural heart, the aortic reservoir, the venous reservoir, and the adjustable clamp. Each component was connected with the Tygon tubing. The circulation loop was filled with water as working fluid. The vibration sensor with the mechanical frequency response up to 500 Hz was mounted near the outlet port of the pump. The output of the roller pump was controlled at 3 L/min and then the output of the centrifugal blood pump was controlled within 2.5 L/min by using the clamp. Considering the rotational speed of the roller pump as the heart rate, we set the rotational speed to the following speeds:

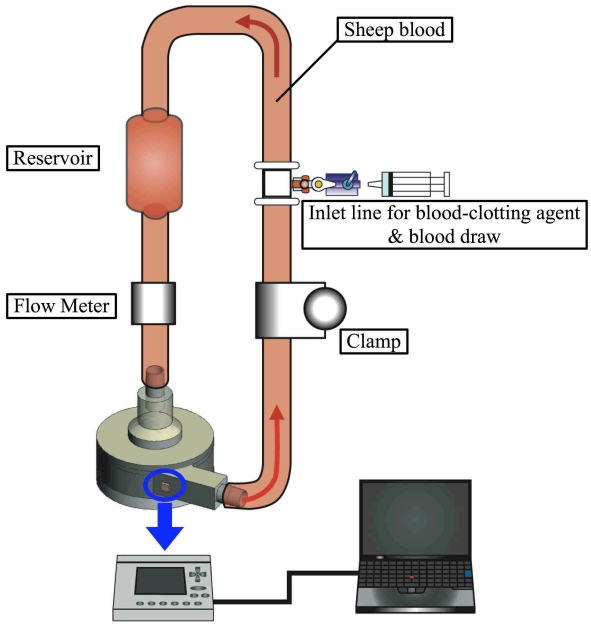

Fig. 6. Mock circulatory loop for the detection of thrombogenesis in the pump

40 beat/min, 80 beat/min, and 120 beat/min. Moreover, the speed of the centrifugal blood pump was set to 2000 rpm. Under the above-mentioned condition, the vibration signals were measured and saved by using the computer via the data recording device at 1 kHz sampling. The data points for FFT were 32768 points. During this experiment, the pressure differences across the centrifugal blood pump were about 90 mmHg on an average.

3) Detection of thrombogenesis in the pump: In this experiment, considering embedding the developed failure detection system into SAH in the future, we applied this system to a centrifugal pump, which has the similar shape of the SAH[7]. Then we performed thrombogenesis detection by using the failure detection system in mock circulatory loop with sheep blood. The mock circulatory loop was constructed as shown in Fig. 6. This mock circulatory loop consists of the reservoir bag, the inlet port, and the centrifugal pump with hydrodynamic bearings (the National Institute of Advanced Science and Technology, Tsukuba, Japan)[5]. The mock circulatory loop was filled with sheep blood as working fluid. The hematocrit of the blood was about 24 %. The acid-citrate-dextrose solution was previously injected into the sheep blood. The vibration sensor with the mechanical frequency response up to 200 Hz was mounted on the side of the pump. The pump flow was set to 5 L/min and the speed pump was set to 2000 rpm. Then pressure differences across the pump were 100 mmHg. To intentionally generate thrombogenesis in the pump, we adjusted activated coagulation time (ACT) with $CaCl_2$.ACT is an index showing the coagulation property of blood. ACT is shown in the range from 0 sec to 1000 sec, as the time showing that the blood congeals. In this experiment, ACT was used to verify whether the failure index detected the prediction of the thrombogenesis in the pump. Under the above-mentioned condition, the vibration signals were saved by using the computer via the data recording device at 400 Hz sampling. The data points for FFT were 16384 points. In order to calculate the failure index, the frequency pattern just before the present frequency pattern was used as the normal standard frequency pattern because the rapid change of the characteristic of the blood was predicted by using $CaCl_2$ as the blood-clotting agent.

III. RESULTS AND DISCUSSION

A. Investigation of frequency pattern affected by pump speed

Fig. 7, shows each frequency pattern based on the vibration signals generated from the centrifugal blood pump at each pump speed. Table I shows the values of the pump flow and the pressure differences across the pump at each of the pump speed. In Fig. 7, the power spectrum intensity was increased at some frequency components at 0-350 Hz when the pump speed increased. Moreover, these frequency ranges shifted to the higher frequency range when the pump speed increased. In general, the continuous blood flow pump has an impeller, therefore we assumed the resonance frequency by the behavior of the impeller was shifted with the increase of the pump speed.

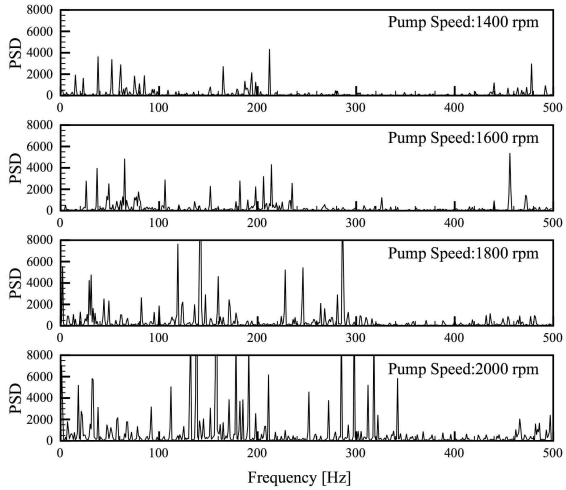

Fig. 7. Frequency patterns of the vibration signal in each pump speed

TABLE I
PUMP FLOW AND PRESSURE DIFFERENCES ACROSS PUMP AT EACH PUMP SPEED

Pump Speed	Pump Flow	Pressure Differenece
1400 rpm	7.2 L/min	15 mmHg
1600 rpm	8.3 L/min	20 mmHg
1800 rpm	9.4 L/min	30 mmHg
2000 rpm	10.5 L/min	40 mmHg

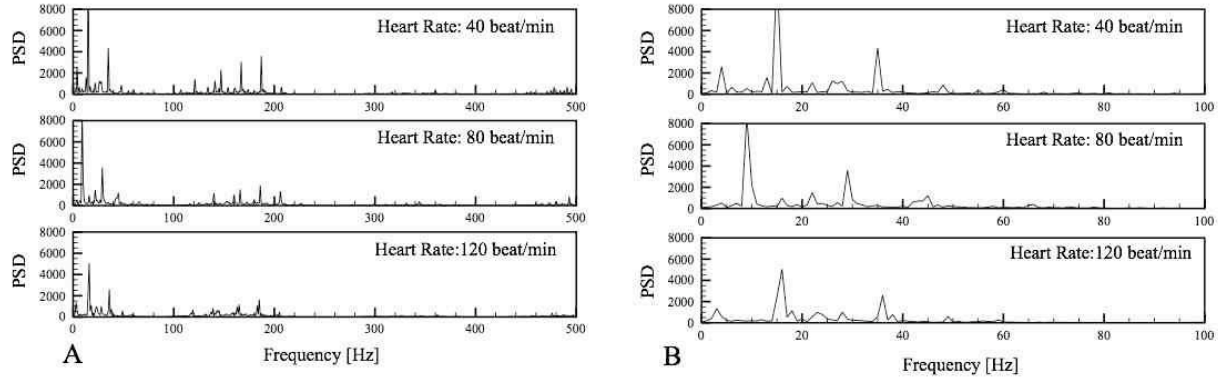

Fig. 8. Frequency patterns of the vibration signal in each heart rate

B. Investigation of the frequency pattern affected by the pulsation

Fig. 8 shows each frequency pattern based on the vibration signals generated from the centrifugal blood pump at the roller pump speeds of 40 beat/min, 80 beat/min, and 120 beat/min. In Fig. 8A, compared to the frequency pattern of 2000 rpm in Fig.7, the power spectrum intensity at 0-50 Hz was stronger because the pulsation of the roller pump affected the mechanical action of the impeller in the centrifugal blood pump. In case of not roller pump but natural heart, it is conceivable that there is not such strong power spectrum intensity. The power spectrum intensity of over 200 Hz in Fig. 7 was stronger than that of over 200Hz in Fig. 8A. It was conceivable that pressure difference across the centrifugal pump and its pump flow affected the power spectrum intensity. In Fig. 8B, the power spectrum of the frequency was shifted to the higher frequency range at 0-50 Hz when the roller pump speed increased. More test would be needed to determined the frequency pattern of the vibration signal affected by the pulsation.

C. Detection of thrombogenesis in the pump

Fig. 9 is the result of this experiment. The dashed lines corresponded with the events shown in Table II. Firstly we focused attention on the time when we drew the blood from the inlet line in Fig. 6 in order to measure ACT. There were four events about the blood draw. The value of the failure index changed greatly at all the events because the motion artifact added to the centrifugal blood pump at the blood draw. Therefore we think it is necessary to distinguish both the vibration signal from the motion artifact and the vibration signal from the pumps as future work. Secondarily we focused attention on the relationship between ACT and the failure index. The failure index and ACT increased at the same when 70 minutes had passed since the experiment started. ACT was greatly different at the event 3 and the event 5. This transition was estimated as follows: By the counteractive injected at the event 1, it became easy for the blood to coagulate and then the blood-coagulating factor was used up to generate thrombus formation in the circulation loop. Therefore ACT was 1000 sec because there was no blood-coagulating factor in the loop. At this time, the failure index showed more than 0.9 after the event 5. This change was supposed that the frequency pattern of the vibration signal was changed by not only the event 5 but also the thrombus formation in the pump. The failure index showed more than 0.8 at the event 4 though the pump current and speed didn't change. Enlarged graph of Fig. 9A from 60 min to 76 min is shown in Fig. 9B. The failure index in event 4 may affected by blood drew in event 3, but the failure index was also supposed to detect the initial sign of thrombogenesis earlier than the pump current and the pump speed. When 80 minutes had passed since the experiment started, we terminated this experiment and checked the impeller. This impeller was shown in Fig.10. We confirmed thrombus formations around this impeller. Moreover the time series data of the frequency pattern were shown in Fig.11. The spectrum intensity increased after 65 minutes when the thrombus formation would be being generated rapidly. This increase of the spectrum intensity was confirmed in all frequency bands.

IV. CONCLUSIONS

In this study, we have developed the failure detection system based on the vibration signals from the artificial

TABLE II
EVENT LIST DURING FAILURE DETECTION TEST FOR THROMBUS FORMATION

No.	Event	ACT [sec]
1	Blood draw* & Counteractive***	206
2	Blood draw**	163
3	Blood draw**	94
4	The failure index over 0.80	
5	Blood draw**	over 1000

* Amount of blood sampling: 10cc
** Amount of blood sampling: 2cc
***Injected quantity: $CaCl_2$ 15ml

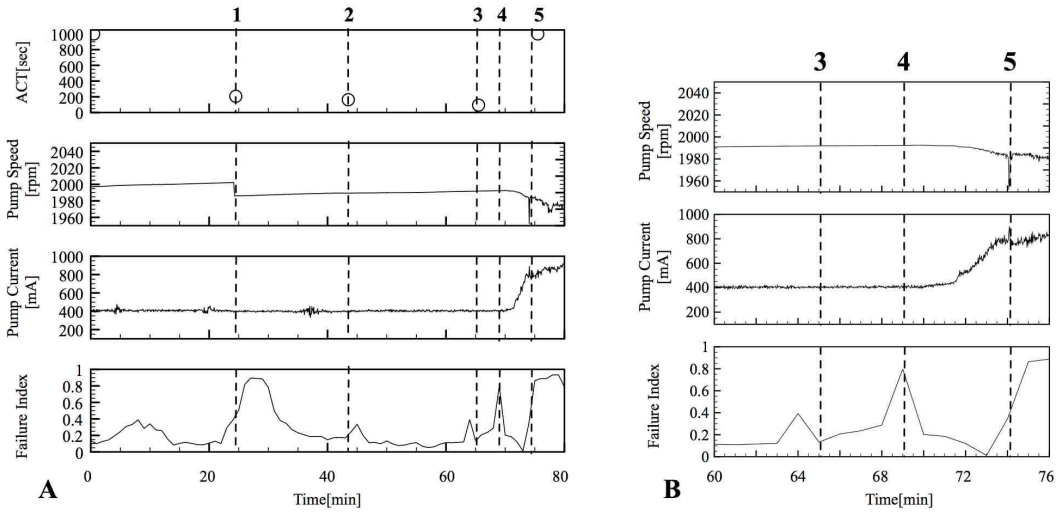

Fig. 9. Time series data under thrombogenesis in the pump

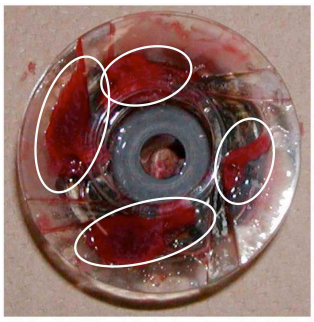

Fig. 10. Thrombus formation around the impeller of the pump in the oval areas

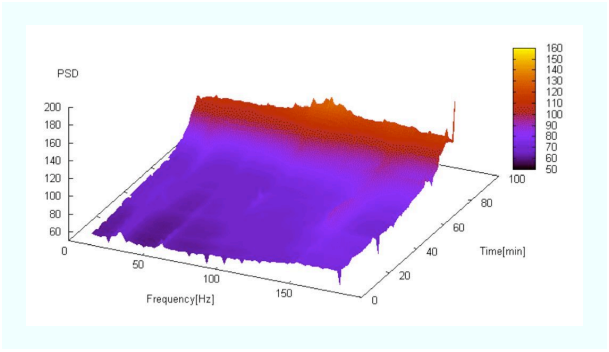

Fig. 11. Time series data of frequency pattern every one minute

hearts in order to enhance the ability of failure detection for the SAH. After confirming that the vibration signal were affected by pump speed and pulsation in two kinds of mock circulatory loops, we performed thrombogenesis detection by using the failure detection system in mock circulatory loop with sheep blood. As a result, this system indicated a possibility of detecting the initial sign of thrombogenesis earlier than the pump current and speed. we confirmed that this system could enhance the ability of failure detection for the SAH. We think that this failure detection system can cooperate with other sensor systems of the SAH and enhance the ability of failure detection for the SAH. In the next step, considering the elimination of motion artifact from the vibration signal, we will apply the developed failure detection system to SAH in animal experiments.

REFERENCES

[1] Yamazaki K, Kihara S, Akimoto T, Tagusari O, Kawai A, Umezu M, Tomioka J, Kormos RL, Griffith BP, Kurosawa H. EVAHEART: an implantable centrifugal blood pump for long-term circulatory support.Jpn J Thorac Cardiovasc Surg. 2002; 50:461-465.

[2] Nose Y and Furukawa K. Current status of the Gyro Centrifugal Blood Pump—Development of the permanently implantable centrifugal blood pump as a biventricular assist device (NEDO Project). Artif Organs 2004; 28:953-958.

[3] Nishinaka T, Schima H, Roethy W, Rajek A, Nojiri C, Wolner E, Wieselthaler GM. The DuraHeart VAD, a magnetically levitated centrifugal pump: the University of Vienna bridge-to-transplant experience. Circ J. 2006 Nov;70:1421-1425.

[4] Yamagishi H, Sankai Y, Yamane T, Jikuya T, and Tsutsui T. Development of built-in type and noninvasive sensor systems for smart artificial heart. ASAIO J. 2003; 49:265-270.

[5] Jammu VB, Malanoski S, Walter T and Smith W. Condition monitoring of rotary blood pumps, ASAIO J. 1997; 43:639-643.

[6] Nakazawa T, Tayama E, Takami Y, Glueck J, Nose Y. In vitro thrombogenesis study in the Gyro C1E3 for vibration assessment. Artif Organs 1997; 21:714-719.

[7] Kosaka R, Yamane T Maruyama, O.; Nishida, M.; Yada, T.; Saito, S.; Hirai, S. Improvement of Hemolysis in a Centrifugal Blood Pump with Hydrodynamic Bearings and Semi-Open Impeller. Engineering in Medicine and Biology Society, 2007. EMBS 2007. 29th Annual International Conference of the IEEE Volume , Issue, 22-26 Aug. 2007 Page(s):3982 - 3985.